

# Structure of $\text{Cs}_{1-x}\text{Rb}_x\text{H}_2\text{PO}_4$ Solid Solutions

V. V. Martsinkevich<sup>a</sup>, V. G. Ponomareva<sup>a</sup>, T. N. Drebushchak<sup>a,b</sup>,  
G. V. Lavrova<sup>b</sup>, and S. S. Shatskaya<sup>a</sup>

<sup>a</sup> Institute of Solid-State Chemistry and Mechanochemistry, Siberian Division, Russian Academy of Sciences, ul. Kutateladze 18, Novosibirsk, 630128 Russia

<sup>b</sup> Novosibirsk State University, ul. Pirogova 2, Novosibirsk, 630090 Russia  
e-mail: ponomareva@solid.nsc.ru

Received June 16, 2009; in final form, December 24, 2009

**Abstract**— $\text{Cs}_{1-x}\text{Rb}_x\text{H}_2\text{PO}_4$  solid solutions have been synthesized for the first time in a broad composition range,  $x = 0.03–0.9$ . At room temperature, the  $\text{Cs}_{1-x}\text{Rb}_x\text{H}_2\text{PO}_4$  solid solutions are isostructural with the low-temperature phase of  $\text{CsH}_2\text{PO}_4$  over the entire composition range studied. In the  $\text{CsH}_2\text{PO}_4$ -based solid-solution series, the unit-cell parameters and volume decrease with increasing Rb content. At high temperatures, the  $\text{Cs}_{1-x}\text{Rb}_x\text{H}_2\text{PO}_4$  solid solutions exist in the range  $x = 0–0.4$ , are isostructural with cubic  $\text{CsH}_2\text{PO}_4$ , and have a smaller unit-cell parameter.

**DOI:** 10.1134/S0020168510070149

## INTRODUCTION

The high-temperature phase of  $\text{CsH}_2\text{PO}_4$  has the highest electrical conductivity ( $6 \times 10^{-2} \text{ S/cm}$ ) among acid salts of alkali metals with the general formula  $\text{M}_n\text{H}_m(\text{XO}_4)_y$  ( $\text{M} = \text{Li}, \text{Na}, \text{K}, \text{Rb}, \text{Cs}, \text{NH}_4$ ;  $\text{X} = \text{S}, \text{Se}, \text{P}, \text{As}$ ). In addition,  $\text{CsH}_2\text{PO}_4$  is one of the most promising medium-temperature electrolytes. However, it undergoes a transition at  $230^\circ\text{C}$  from a high-temperature, cubic phase to a low-temperature, monoclinic phase, accompanied by a drop in electrical conductivity by four orders of magnitude.

One common way of modifying the transport properties of ionic salts is by doping. In particular, the effect of both cation ( $\text{Li}^+$ ,  $\text{K}^+$ ,  $\text{Rb}^+$ ) and anion ( $\text{H}_2\text{PO}_4^-$ ) substitutions in  $\text{CsHSO}_4$  on the phase composition of the resulting materials has been studied in a wide concentration range [1–5]. In a number of compositions, stabilization of an amorphous state was observed (e.g., in  $\text{Cs}_{0.67}\text{K}_{0.33}\text{HSO}_4$ ) or individual phases with other crystal structures were formed:  $\text{Cs}_3(\text{H}_2\text{PO}_4)(\text{HSO}_4)_2$ ,  $\text{Cs}_2(\text{H}_2\text{PO}_4)(\text{HSO}_4)$ ,  $\text{CsNa}_2(\text{HSO}_4)_3$ , and  $\text{Cs}_2\text{Na}(\text{HSO}_4)_3$  [6].

In contrast to what occurs in  $\text{CsHSO}_4$ , partial  $\text{NH}_4^+$  substitution for  $\text{Cs}^+$  in  $\text{CsH}_2\text{PO}_4$  causes neither amorphization of the salt nor formation of other phases [7]. There are two  $\text{Cs}_{1-x}(\text{NH}_4)_x\text{H}_2\text{PO}_4$  solid-solution phases, one based on the low-temperature, monoclinic phase of  $\text{CsH}_2\text{PO}_4$  ( $0 \leq x < 0.1$ ), and the other on the low-temperature, tetragonal phase of  $\text{NH}_4\text{H}_2\text{PO}_4$  ( $0.4 < x \leq 1$ ), which is caused by the structural distinction between the end-members. In the intermediate composition range,  $0.1 < x < 0.4$ , no solid solutions exist. In addition, cation substitutions were shown to

influence the phase transition of  $\text{CsH}_2\text{PO}_4$  and its chemical stability in the superionic state. The monoclinic phase undergoes a phase transition to the cubic, superionic phase, whose temperature decreases with increasing  $\text{NH}_4^+$  concentration, by up to  $10^\circ\text{C}$  during heating and by up to  $37^\circ\text{C}$  during cooling, whereas the tetragonal phase ( $x > 0.4$ ) undergoes no superionic transition up to its melting point, just like the unsubstituted salt  $\text{NH}_4\text{H}_2\text{PO}_4$ .

$\text{RbH}_2\text{PO}_4$ , yet another salt of this family, is known to have a high-temperature form with a superionic transition temperature of  $280^\circ\text{C}$  [8].  $\text{CsH}_2\text{PO}_4$ -based double salts containing other alkali-metal cations have not been systematically studied. In this paper, we report the synthesis of  $\text{Cs}_{1-x}\text{Rb}_x\text{H}_2\text{PO}_4$  double salts in a wide composition range and a detailed study of their structure.

According to X-ray diffraction (XRD) data,  $\text{CsH}_2\text{PO}_4$  has a monoclinic ( $P2_1/m$ ) structure at room temperature, with unit-cell parameters  $a = 7.9122 \text{ \AA}$ ,  $b = 6.3831 \text{ \AA}$ ,  $c = 4.8803 \text{ \AA}$ ,  $\beta = 107.73^\circ$ ,  $V = 250.19 \text{ \AA}^3$ ,  $Z = 2$  [9]. Its low-temperature phase has a two-dimensional hydrogen-bond network, in which the  $\text{PO}_4$  tetrahedra are linked by both asymmetric (one energy minimum) and symmetric (two minima) hydrogen bonds. The phosphate tetrahedra are linked into chains by short hydrogen bonds,  $2.47 \text{ \AA}$  in length, and the chains are linked into two-dimensional layers by longer hydrogen bonds,  $2.54 \text{ \AA}$  in length. The high-temperature phase crystallizes in cubic symmetry ( $Pm3m$ ), with  $a = 4.9613 \text{ \AA}$ ,  $V = 122.1 \text{ \AA}^3$ , and  $Z = 1$  [10]. At the center of each unit cell, there is an ideal  $\text{PO}_4$  tetrahedron disordered in six equally probable positions. Accordingly, hydrogen bonds may have six directions. The cesium atoms are located at the corners of the unit cell.

**Table 1.** Unit-cell parameters of low-temperature  $\text{Cs}_{1-x}\text{Rb}_x\text{H}_2\text{PO}_4$ 

$x$	$a, \text{\AA}$	$b, \text{\AA}$	$c, \text{\AA}$	$\beta, \text{deg}$
0	7.912(2)	6.384(4)	4.886(6)	107.84(4)
0.03	7.9056(8)	6.374(2)	4.875(2)	107.82(2)
0.1	7.892(2)	6.371(5)	4.876(7)	108.01(5)
0.3	7.845(1)	6.332(3)	4.858(5)	108.09(3)
0.4	7.834(2)	6.320(4)	4.851(7)	108.03(5)
0.6	7.786(2)	6.267(3)	4.818(5)	108.19(4)
0.9	7.62(3)	6.23(1)	4.75(2)	108.1(3)

$\text{RbH}_2\text{PO}_4$  has a tetragonal ( $I4_2d$ ) structure at room temperature and a monoclinic ( $P2_1/a$ ) structure, similar to that of low-temperature  $\text{CsH}_2\text{PO}_4$ , above 79°C [11].

## EXPERIMENTAL

$\text{Cs}_{1-x}\text{Rb}_x\text{H}_2\text{PO}_4$  ( $x = 0\text{--}0.6$ ) single crystals were grown from aqueous solutions containing appropriate ratios of phosphoric acid, cesium carbonate, and rubidium carbonate by room-temperature evaporation. The crystals were washed with acetone and calcined at 150°C for 2 h in order to remove the residual water. Polycrystalline  $\text{Cs}_{1-x}\text{Rb}_x\text{H}_2\text{PO}_4$  ( $x = 0.8\text{--}0.9$ ) samples were prepared by reacting appropriate mixtures at 200°C. The cation composition of the samples was determined by a combination of atomic absorption and emission flame photometry ( $\lambda = 852.1 \text{ nm}$ ) [12].  $\text{H}_2\text{PO}_4^-$  was determined by differential colorimetry as the yellow vanadomolybdate complex [13]. From the chemical analysis and XRD data, the accuracy in the compositions obtained was estimated at 3–5%.

Powder XRD patterns were collected on DRON-3 ( $\text{Cu}K_{\alpha}$  radiation,  $\lambda = 1.5418 \text{ \AA}$ ) and Bruker D8-GADDS ( $\text{Cu}K_{\alpha}$  radiation,  $\lambda = 1.5418 \text{ \AA}$ , graphite monochromator, 0.5-mm receiving slit, area detector) diffractometers. High-temperature XRD measurements were made on a Stoe MP powder diffractometer ( $\text{Cu}K_{\alpha_1}$  radiation,  $\lambda = 1.5406 \text{ \AA}$ , bent germanium monochromator, linear position-sensitive detector) equipped with a high-temperature attachment (transmission geometry, 0.5-mm-diameter capillary).

Unit-cell parameters were determined from 11 independent reflections using the IK program [14].

## RESULTS AND DISCUSSION

According to XRD data, the structures of the individual salts  $\text{CsH}_2\text{PO}_4$  and  $\text{RbH}_2\text{PO}_4$  were similar to those reported earlier [9, 11].

Figure 1 shows the XRD patterns of  $\text{Cs}_{1-x}\text{Rb}_x\text{H}_2\text{PO}_4$  double salts of various compositions. The structure of low-temperature  $\text{CsH}_2\text{PO}_4$  is seen to persist in the double salts up to  $x = 0.9$ . The relative XRD intensities vary little, and the reflections gradually shift to larger angles, indicating the formation of  $\text{CsH}_2\text{PO}_4$ -based solid solutions with reduced unit-cell parameters. Table 1 lists the unit-cell parameters of  $\text{Cs}_{1-x}\text{Rb}_x\text{H}_2\text{PO}_4$  with  $x = 0\text{--}0.9$  (calculations with the IK program). The low-temperature phase of the synthesized  $\text{CsH}_2\text{PO}_4$  has a monoclinic ( $P2_1/m$ ) structure with lattice parameters  $a = 7.912(2) \text{ \AA}$ ,  $b = 6.384(4) \text{ \AA}$ ,  $c = 4.886(6) \text{ \AA}$ , and  $\beta = 107.84(4)^\circ$  ( $V = 234.96 \text{ \AA}^3$ ), in agreement with those reported by Matsunaga et al. [9]. The low-temperature phase of the synthesized  $\text{RbH}_2\text{PO}_4$  has a tetragonal ( $I4_2d$ ) structure with lattice parameters  $a = 7.611(1) \text{ \AA}$  and  $c = 7.301(3) \text{ \AA}$ , in agreement with those reported by Rusakov and Kheiker [11].

As seen in Figs. 2–4, the lattice periods and unit-cell volume decrease with increasing Rb content, whereas  $\beta$  increases. The change in  $c$  parameter is slightly smaller than those in  $a$  and  $b$ . These changes lead to a reduction in the difference in length between the hydrogen bonds along the  $a$  and  $c$  axes. As seen in Figs. 2 and 3, the unit-cell parameters and 011 interplanar spacing are linear functions of  $\text{Rb}^+$  content, in accordance with Vegard's law.

Thus, as distinct from  $\text{Cs}_{1-x}(\text{NH}_4)_x\text{H}_2\text{PO}_4$ , solid solutions  $\text{Cs}_{1-x}\text{Rb}_x\text{H}_2\text{PO}_4$  exist over the entire composition range. Note that the solid solutions were obtained by different procedures: via both coprecipitation from aqueous solutions and heating of mechanical

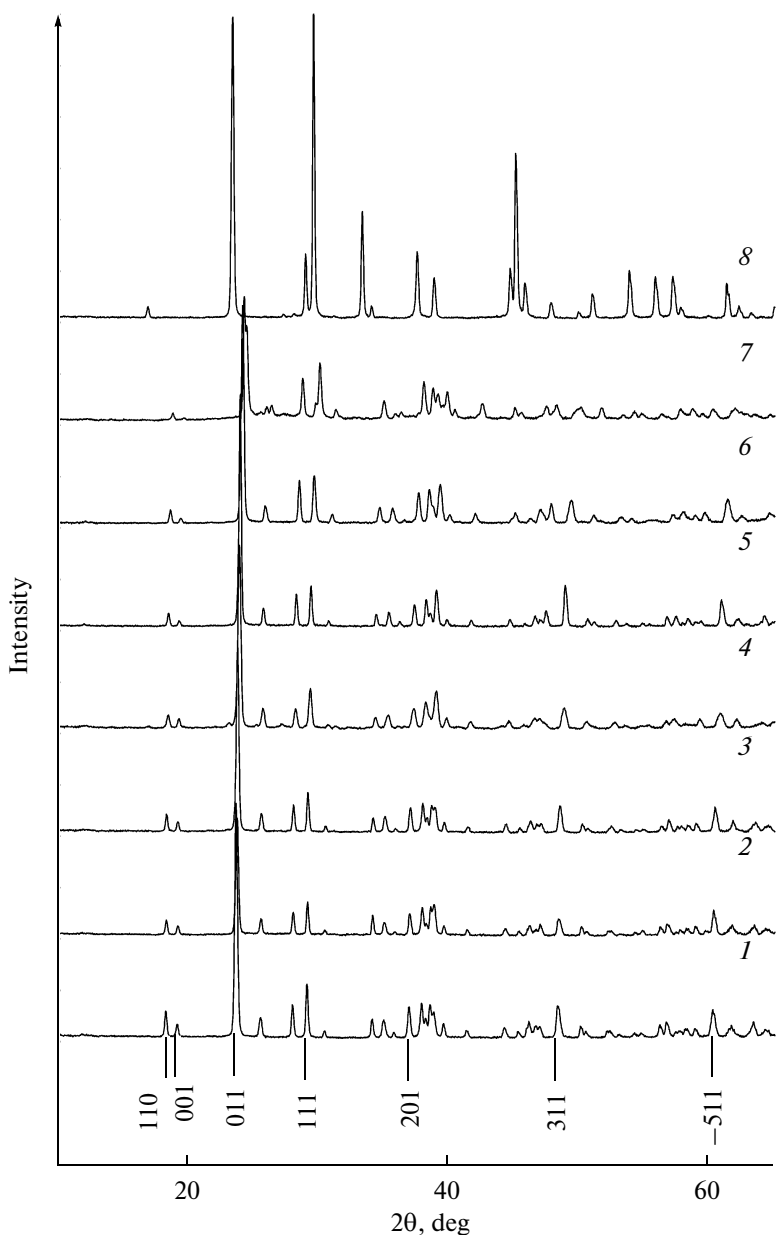


**Fig. 1.** XRD patterns of (1)  $\text{CsH}_2\text{PO}_4$ , (2–7)  $\text{Cs}_{1-x}\text{Rb}_x\text{H}_2\text{PO}_4$ , and (8)  $\text{RbH}_2\text{PO}_4$ ;  $x = (2) 0.03, (3) 0.1, (4) 0.3, (5) 0.4, (6) 0.6, (7) 0.9$ .

mixtures to 200°C. As seen in Fig. 1, the solid-solution range extends up to  $x = 0.9$ . At  $x = 0.9$ , however, the unit-cell parameters were determined from XRD data with a substantially higher uncertainty than those at lower  $x$  values, probably because the  $x = 0.9$  sample was more hygroscopic, which broadened the reflections from it and reduced their intensity.

Isomorphic substitutions are known to be more likely when the atoms involved have the same coordination number and, in the case of covalent compounds, when they are identical in bonding configuration. At a given temperature and pressure, the degree of isomorphism is determined by the proximity in interatomic distances,

chemical bonding, and the electronic structure of the atoms. If substituents differ considerably in cation radius, the structure of solid solutions between acid salts typically differs markedly from those of the end-members [1, 5, 6]. The likely reason for the large width of the solid-solution range is that rubidium dihydrogen phosphate undergoes a transition at 79°C to a monoclinic phase similar in structure to low-temperature  $\text{CsH}_2\text{PO}_4$  and also that the difference in ionic radius between Cs and Rb is not very large ( $\text{Cs}^+$ , 1.74 Å;  $\text{Rb}^+$ , 1.61 Å;  $\text{NH}_4^+$ , 1.42 Å).

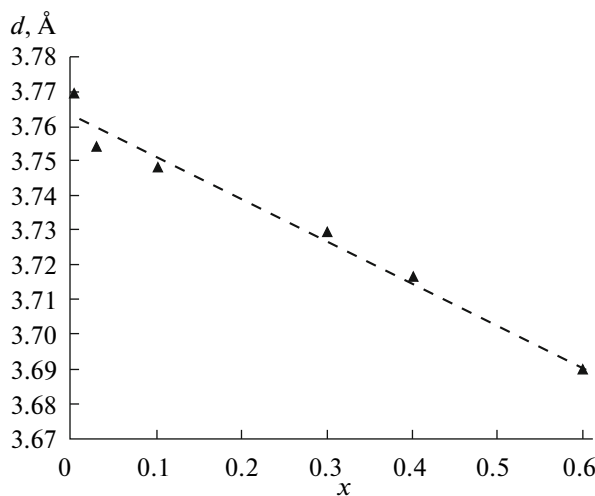


Fig. 2. 011 interplanar spacing as a function of Rb content for  $\text{Cs}_{1-x}\text{Rb}_x\text{H}_2\text{PO}_4$ .

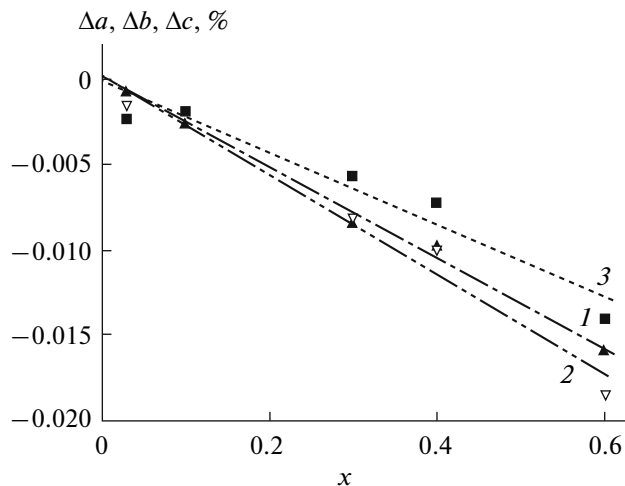


Fig. 3. Composition dependences of relative changes in the unit-cell parameters (1)  $a$ , (2)  $b$ , and (3)  $c$  of  $\text{Cs}_{1-x}\text{Rb}_x\text{H}_2\text{PO}_4$ .

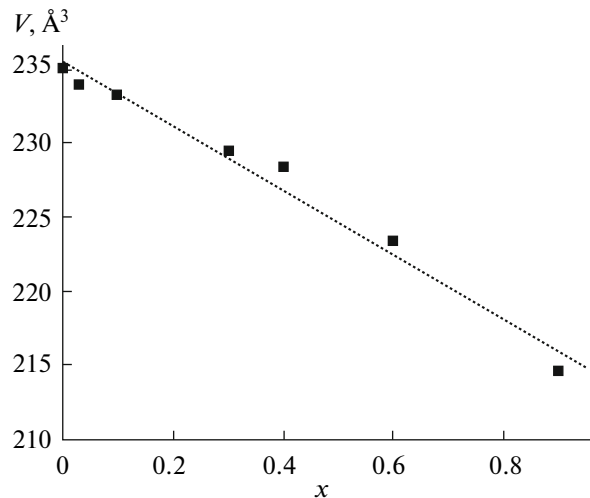


Fig. 4. Composition dependence of the unit-cell volume for  $\text{Cs}_{1-x}\text{Rb}_x\text{H}_2\text{PO}_4$ .

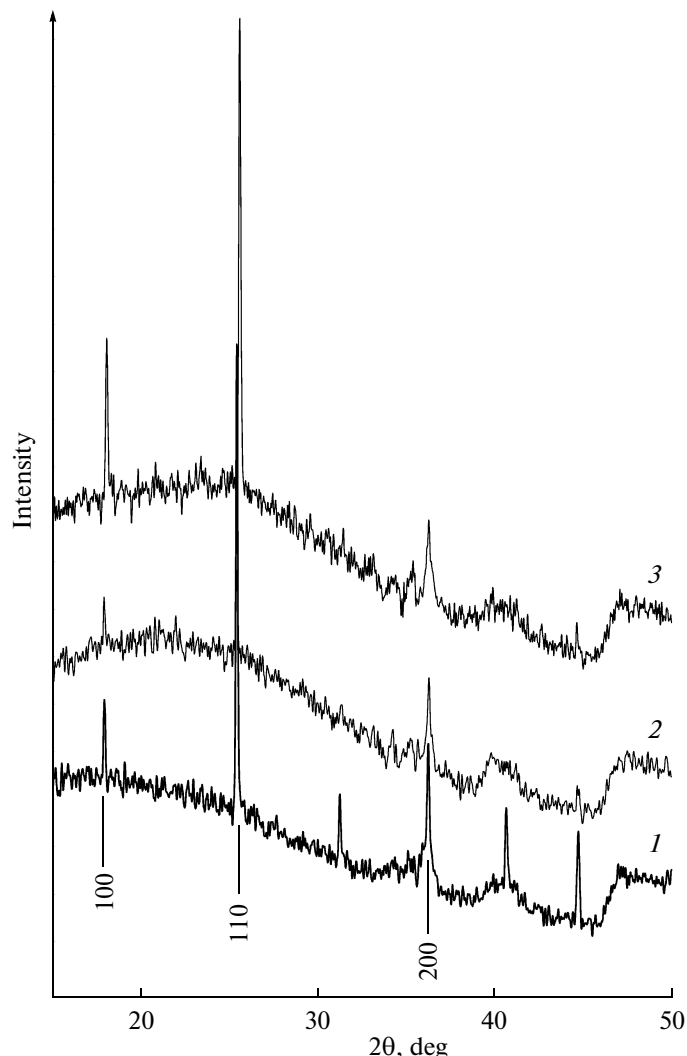


Fig. 5. XRD patterns of high-temperature  $\text{Cs}_{1-x}\text{Rb}_x\text{H}_2\text{PO}_4$  with  $x = (1) 0.01$ , (2) 0.2, and (3) 0.4 ( $t = 240^\circ\text{C}$ ).

As shown earlier, at  $230^\circ\text{C}$   $\text{Cs}_{0.97}\text{Rb}_{0.03}\text{H}_2\text{PO}_4$  is isostuctural with the high-temperature, superionic phase of  $\text{CsH}_2\text{PO}_4$  but has slightly smaller unit-cell parameters [15]. The high-temperature XRD data for the superionic phase of  $\text{Cs}_{1-x}\text{Rb}_x\text{H}_2\text{PO}_4$  with  $x = 0.1$ , 0.2, and 0.4 at  $240^\circ\text{C}$  also indicate the formation of solid solutions based on high-temperature  $\text{CsH}_2\text{PO}_4$ , with a gradual reduction in  $a$  (Fig. 5). Their unit-cell parameters are listed in Table 2. For  $x \leq 0.4$ , the transition to the high-temperature, superionic phase, isomorphic with  $\text{CsH}_2\text{PO}_4$ , occurs in the temperature range  $220$ – $235^\circ\text{C}$ . Partial rubidium substitution for cesium and the formation of solid solutions, of course, influence the transport and thermodynamic properties of the double salts and the hydrogen bond energetics in them, which will be considered in a subsequent communication.

**Table 2.** Unit-cell parameters of high-temperature  $\text{Cs}_{1-x}\text{Rb}_x\text{H}_2\text{PO}_4$  at 240°C

$x$	$a, \text{\AA}$	$V, \text{\AA}^3$
0	4.961	122.10
0.1	4.9561(1)	121.74
0.2	4.952(2)	121.43
0.4	4.946(8)	120.96

## CONCLUSIONS

We synthesized  $\text{Cs}_{1-x}\text{Rb}_x\text{H}_2\text{PO}_4$  double salts in a broad composition range and investigated their structural properties. At 25°C, the double salts with  $x = 0.03\text{--}0.9$  are isostructural with low-temperature cesium dihydrogen phosphate and have smaller  $a$ ,  $b$ , and  $c$  cell parameters. At high temperatures, the  $\text{Cs}_{1-x}\text{Rb}_x\text{H}_2\text{PO}_4$  solid solutions are isostructural with cubic cesium dihydrogen phosphate and exist in the range  $x = 0\text{--}0.4$ .

## ACKNOWLEDGMENTS

We are grateful to S.V. Tsibulya for his assistance with the structure calculations.

This research was supported in part by the Russian Foundation for Basic Research, grant no. 07-03-12151.

## REFERENCES

- Mhiri, T. and Colomban, Ph., Defect-Induced Smoothing of the Superionic Phase Transition in  $\text{Cs}_{1-x}\text{M}_x\text{HSO}_4$  Protonic Conductors: I. Potassium Substitution, *Solid State Ionics*, 1991, vol. 44, pp. 215–225.
- Mhiri, T., Daoud, A., and Colomban, Ph., Defect-Induced Smoothing of the Superionic Phase Transition in  $\text{Cs}_{1-x}\text{M}_x\text{HSO}_4$  Protonic Conductors: II. Lithium Substitution, *Solid State Ionics*, 1991, vol. 44, nos. 3–4, pp. 227–234.
- Mhiri, T., Daoud, A., and Colomban, Ph., Defect-Induced Smoothing of the Superionic Phase Transition in  $\text{Cs}_{1-x}\text{M}_x\text{HSO}_4$  Protonic Conductors. III. Rubidium Substitution, *Solid State Ionics*, 1991, vol. 44, nos. 3–4, pp. 235–243.
- Haile, S.M., Lentz, G., Kreuer, K.-D., and Maier, J., Superprototypic Conductivity in  $\text{Cs}_3(\text{HSO}_4)_2(\text{H}_2\text{PO}_4)$ , *Solid State Ionics*, 1995, vol. 77, pp. 128–134.
- Chisholm, C.R.I. and Haile, S.M., Superprototypic Behavior of  $\text{Cs}_2(\text{HSO}_4)(\text{H}_2\text{PO}_4)$ —A New Solid Acid in the  $\text{CsHSO}_4\text{--CsH}_2\text{PO}_4$  System, *Solid State Ionics*, 2000, vols. 136–137, pp. 229–241.
- Chisholm, C.R.I., Cowan, L.A., Haile, S.M., and Klooster, W.T., Synthesis, Structure, and Properties of Compounds in the  $\text{NaHSO}_4\text{--CsHSO}_4$  System: 1. Crystal Structures of  $\text{CsNa}_2(\text{HSO}_4)_3$  and  $\text{Cs}_2\text{Na}(\text{HSO}_4)_3$ , *Chem. Mater.*, 2001, vol. 13, pp. 2574–2583.
- Baranov, A.I., Grebenev, V.V., Khodan, A.N., et al., Optimization of Superionic Acid Salts for Fuel Cell Applications, *Solid State Ionics*, 2005, vol. 176, pp. 2871–2874.
- Rapoport, E., Clark, J.B., and Richter, P.W., High-Pressure Phase Relations of  $\text{RbH}_2\text{PO}_4$ ,  $\text{CsH}_2\text{PO}_4$ , and  $\text{KD}_2\text{PO}_4$ , *J. Solid State Chem.*, 1978, vol. 24, nos. 3–4, pp. 423–433.
- Matsunaga, H., Itoh, K., and Nakamura, E., X-Ray Structure Study of Ferroelectric Cesium Hydrogen Phosphate at Room Temperature, *J. Phys. Soc. Jpn.*, 1980, vol. 48, pp. 2011–2014.
- Preisinger, A., Mreiter, K., and Bronowska, W., The Phase Transition of  $\text{CsH}_2\text{PO}_4$  (CDP) at 505 K, *Mater. Sci. Forum*, 1994, vols. 166–169, pp. 511–516.
- Rusakov, A.A. and Kheiker, D.M., Room-Temperature Structure Refinement of  $\text{RbH}_2\text{PO}_4$ , *Kristallografiya*, 1978, vol. 23, no. 2, pp. 409–411.
- Stolyarova, I.A. and Filatova, M.F., *Atomno-absorbsionnaya spektrometriya* (Atomic Absorption Spectroscopy), Leningrad: Nedra, 1981, p. 24.
- Ognina, V.A., *Metody khimicheskogo analiza fosfatnykh rud* (Chemical Analysis of Phosphate Ores), Morkovskaya, G.A., Ed., Moscow: Goskhimizdat, 1961.
- Solov'eva, L.P., Tsibulya, S.V., and Zabolotnyi, V.A., “*Polikristall*—sistema programm dlya strukturnykh raschetov
- (Polikristall—A Software Package for Structural Calculations), Novosibirsk: Inst. Kataliza Sib. Otd. Ross. Akad. Nauk, 1988, p. 122.
- Lavrova, V.G., Martsinkevich, V.V., and Ponomareva, V.G., Electrical and Thermodynamic Properties of  $\text{Cs}_{0.97}\text{Rb}_{0.03}\text{H}_2\text{PO}_4$ , *Neorg. Mater.*, 2009, vol. 45, no. 7, pp. 857–863 [*Inorg. Mater.* (Engl. Transl.), vol. 45, no. 7, pp. 795–801].